

Competition of Spin-Fluctuations and Phonons in Superconductivity of ZrZn_2

D.J. Singh and I.I. Mazin

Center for Computational Materials Science,
Naval Research Laboratory, Washington, DC 20375, U.S.A.

(November 1, 2018)

It has been long suspected that spin fluctuations in the weak itinerant ferromagnet ZrZn_2 may lead to a triplet superconductivity in this material. Here we point out another possibility, a spatially inhomogeneous singlet superconducting state (a Fulde-Ferrell-Larkin-Ovchinnikov state). We report detailed electronic structure calculations, as well as calculations of the zone center phonons and their coupling with electrons. We find that the exchange splitting is nonuniform and may allow for gap formation at some parts of the Fermi surface. We also find that there is substantial coupling of Zr rattling modes with electrons, which can, in principle, provide the necessary pairing in the s-channel.

The recent discovery of superconductivity in the ferromagnetic phase of ZrZn_2 [1] has revived interest in this unusual compound. ZrZn_2 has traditionally been considered a prototypical example of a weak itinerant (Stoner) ferromagnet. Very small magnetic moments (values from 0.12 to 0.23 μ_B) have been reported. These do not saturate even at magnetic fields as high as 35 T, indicating softness of the magnetic moment amplitude and suggesting existence of soft longitudinal spin fluctuations. Already in the first report of ferromagnetism [2] it was pointed out that ZrZn_2 may be a ferromagnetic superconductor, of the type discussed earlier by Ginzburg [3]. Later the idea of triplet spin-fluctuation induced superconductivity in ferromagnetic ZrZn_2 was theoretically elaborated by Fay and Appel [4]. However, experimental searches for superconductivity in ZrZn_2 [5] were unsuccessful, till now. It is therefore very tempting to identify ZrZn_2 as a triplet superconductor. This is supported by the fact that superconductivity seems to disappear with pressure at about the same point where the magnetic Curie temperature goes to zero. On the other hand, the low superconducting fraction does not allow accurate determination of the critical pressure for the superconducting transition to clearly show that it coincides with that for the magnetism. Thus one cannot fully exclude the possibility that the two types of orders are spatially separated. Still, it is likely that they do coexist, and if so, a key question is whether their interaction is constructive or destructive. A definite answer will require more study. However, before making any theoretical speculations one needs to get a detailed understanding of the electronic structure of this compound, and its relation with superconductivity and magnetism. Here we present an accurate analysis of the para- and ferromagnetic electronic structure and identify what seems to be the most interesting and relevant features of the band structure for superconductivity.

We find that, despite the very small magnetization, the rigid band model is inappropriate for ZrZn_2 . The

exchange splitting, $\Delta_{xc}(\mathbf{k})$, differs from band to band by more than a factor of two. Even more importantly, some bands have extremely small ($\Delta k \approx 0.12 \text{ \AA}^{-1}$) exchange splitting in k -space, making superconductivity in these bands less sensitive to magnetic ordering. Furthermore, the calculated Fermi surface shows substantial nesting features, suggesting that antiferromagnetic fluctuations may play a role in superconductivity. Finally, we found that the rattling Zr modes are soft and couple strongly with electrons. We emphasize that, while triplet superconductivity is an interesting possibility, the facts are nevertheless compatible with an inhomogeneous Fulde-Ferrell-Larkin-Ovchinnikov (FFLO) state [7] of the s-wave symmetry as well.

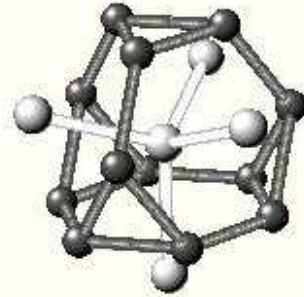


FIG. 1. Coordination of a Zr atom in ZrZn_2 .

ZrZn_2 occurs in a C15 crystal structure, where the Zr forms a diamond-type lattice, and the Zn forms a network of corner-sharing tetrahedra (another way to visualize this structure is to imagine a spinel without anions). An interesting aspect is the “overcoordination” of Zr: it has 16 nearest neighbors consisting of 12 Zn, forming a truncated tetrahedron (Fig.1), at a distance (at $T=50\text{K}$ [8]) 5.745 a.u., and 4 Zr at 6.001 a.u. The latter approximately corresponds to the bond length in Zr metal. Since the metallic radius of Zn is 16% smaller than that of Zr, Zr and Zn do not form strong bonds. On the other hand, Zr, unlike carbon, does not form highly directional bonds, so 4 Zr-Zr bonds in ZrZn_2 do not provide strong bonding

either. This makes Zr “rattling” rather soft. At the same time, Zn has 8 neighbors at a distance 4.9 a.u., noticeably *less* than in Zn metal (5.04 – 5.51 a.u.). Correspondingly, one expect that Zn bond-stretching vibrations should be relatively hard.

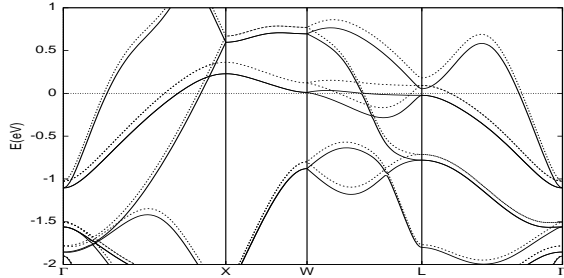


FIG. 2. LSDA band structure of ZrZn_2 . E_F is at 0. Solid (dashed) lines show majority (minority) bands corresponding to the magnetization of $0.2 \mu_B/\text{f.u.}$

We calculated the band structure of both para- and ferromagnetic ZrZn_2 , using the experimental lattice parameter of 13.858 a.u. [8]. The calculations were done in the local spin density approximation (LSDA) [9] with the general potential linearized augmented planewave (LAPW) method. [10]. Well converged zone samplings and basis sets, including local orbitals [11] to treat the semicore states and relax linearization errors, were used. The spin-polarized band structure is shown in Fig.2. The Fermi surface is shown in Fig.3. Our calculations agree well with those published before (Refs. [12,13] and references therein). The basic electronic characteristics of the nonmagnetic electronic structure are: density of states at the Fermi level, $N(E_F) = 2.43$ states/eV spin f.u., Fermi velocity, $v_F = 2.5 \times 10^7$ cm/sec, plasma frequency, $\omega_{pl} = 4.0$ eV, Hall concentration 5×10^{22} e/cm³ [14]. The bands near the Fermi level can be described in the first approximation as originating from the bonding combination of the t_{2g} Zr orbitals (the electronic sphere and the electronic rounded dodecahedron, both around the Γ point), and the bonding e_g orbitals (the “interconnected pancakes”). The tubular network Fermi-surface is a hybridized combination of both types of states. However, such a view is oversimplified. Comparing the width of the d -band of ZrZn_2 , and of the pure Zr sublattice (with Zn removed), we observe that the band width of the latter is about 30% smaller. Using the well-known nearest-neighbor tight binding formula, we see that $W_{\text{ZrZn}_2} \approx \sqrt{4t_{\text{Zr-Zr}}^2 + 12t_{\text{Zr-Zn}}^2}$, which gives a rough estimate of $t_{\text{Zr-Zn}} \sim 0.5t_{\text{Zr-Zr}}$, not surprising, given the smaller radius of Zn.

Although the effect of Zn on the total band width is relatively small (cf. with the fcc Zr with the same Zr-Zr distance, which has twice larger bandwidth, $W_{\text{Zr-fcc}} \approx \sqrt{12t_{\text{Zr-Zr}}^2}$ [15]), it is not negligible, and, interestingly, it is nonuniform over the Brillouin zone. Specifically, the

electron surface around the Γ point has more than 50% Zn character, while the other bands have nearly everywhere less than 20% of it (Fig.3) [16]. This leads, in turn, to nonuniform exchange splitting $\Delta_{xc}(\mathbf{k})$ (Fig.3). For the Fermi surface near the Γ point, the splitting of the Fermi surface is extremely small, $\delta k_F \approx 0.017 \text{ \AA}^{-1}$. The FFLO period, $2\pi/\delta k_F \approx 360 \text{ \AA}$, is long enough to allow for superconductivity in this band with a coherence length $\xi \sim 290 \text{ \AA}$ (according to Ref. [1]). This band has an exceptionally small δk_F , but the other bands have small δk_F as well. In fact, for the most of the Fermi surface $\delta k_F \lesssim 0.07 \text{ \AA}^{-1}$, corresponding to $2\pi/\delta k_F \approx 90 \text{ \AA}$.

The spin-polarized bands, used to produce the lower panel of Fig.3, are shown in Fig.2. These were calculated by fixing the total magnetization to be $0.2 \mu_B/\text{f.u.}$ Fully relaxed calculations converge to the value of $0.7 \mu_B/\text{f.u.}$, nearly 4 times larger than the accepted experimental value of $0.17\text{-}0.20 \mu_B/\text{f.u.}$ This is somewhat unexpected, for usually correlation effects, not completely accounted for in LSDA, tend to *increase* the tendency to magnetism. It may be that the actual samples are spatially inhomogeneous, with magnetic and nonmagnetic (and possibly superconducting) regions. Alternatively, the LSDA may overestimate tendency to magnetism in this material for some unknown reason.

In vicinity of an itinerant ferromagnetic critical point, theory predicts a triplet superconductivity, with T_c first growing as one moves in either direction from the critical point, and then decaying as the spin fluctuations become weaker in either nonmagnetic, or ferromagnetic phases. Such a behavior has been observed on the ferromagnetic side, for instance, in UGe_2 , and it was suggested that the difference between the longitudinal spin fluctuation spectra in the para- and ferromagnetic phases makes superconductivity much weaker and thus unobservable on the paramagnetic side [17]. So, a triplet state remains a plausible explanation for the superconductivity in ZrZn_2 . We want to call attention, however, to another possibility, namely an FFLO inhomogeneous s-wave superconducting state. Both models can successfully explain the major experimental observations [1]: high sensitivity to sample purity (impurity scattering would make the superconducting electrons from a band with a small exchange splitting feel a large splitting of the other bands), absence of a specific heat jump (the Fermi surface sections with a large splitting may have vanishing gaps), disappearance of superconductivity near the FM critical point (because of the pair-breaking effect of spin fluctuations). An apparent difference between the two models is that in the latter superconductivity not only is restored at pressures higher than critical (this is true for most models of the triplet superconductivity as well), but also, generically, T_c grows much faster on the paramagnetic side than on the ferromagnetic one. The high pressure data reported in Ref. [1] do not extend far enough beyond the critical point and do not give a definite answer

to whether superconductivity reappears at higher pressures or not. Unless the strongly interacting Zr rattling modes would harden substantially, and/or lose their coupling with electrons, under pressure, the FFLO scenario suggests superconductivity re-entrance at a pressure high enough to suppress the spin fluctuations. We did check the pressure dependence of the T_{2g} mode, and found that under a 3% volume compression it stiffens by 11%, while it softens by 6% under a 3% expansion.

A major question that arises in connection with this alternative is, what would be the pairing interaction behind the assumed s-wave state? It needs to be sufficiently strong to make an FFLO state energetically competitive. To gain more insight in that, we performed lattice dynamics calculations for the zone center optical modes [18]. There are 15 such modes at 6 distinctive frequencies: 4 triple-degenerate modes of T_{1u} (two), T_{2u} , and T_{2g} modes, one double-degenerate E_u mode, and one non-degenerate A_{1u} mode (Table 1). The two softest modes are particularly interesting. Physically, they correspond to “rattling” motion of Zr inside the Zn cage, hence their softness and the small difference in their frequencies. Since these two modes join at the zone boundary, one can see that they have little dispersion, as is common for rattling modes. The even (T_{2g}) mode is the only one that can couple with phonons at the Γ point; but as these two modes are essentially local vibrations, they presumably couple with about the same strength for general wave vectors, so the coupling constant computed for a T_{2g} mode should be a reasonable estimate for the coupling constants of all six rattling T_{2g} and T_{1u} phonons.

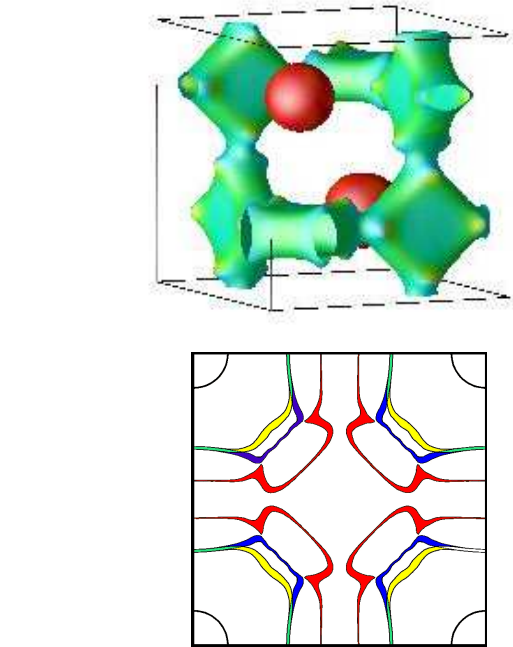
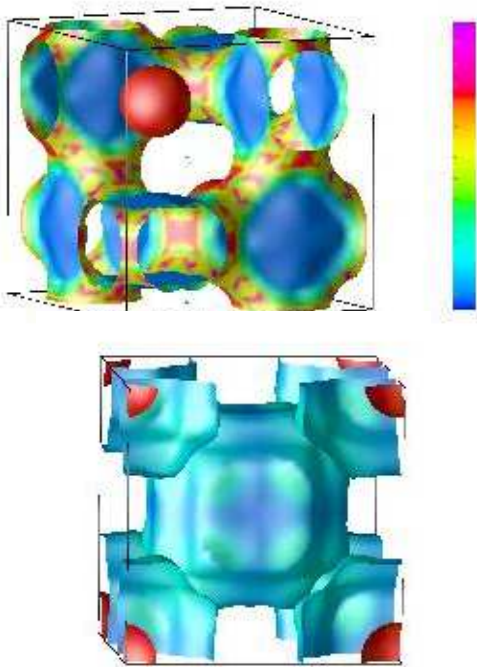


FIG. 3. Fermi surface of ZrZn_2 . The three upper figures show the nongnatic Fermi surfaces, colored by the relative percentage of Zn character. The color bar goes from 5% to 60%. The bands shown are, from up down: bands 1 and 2 (Γ -points at the corners), bands 1 and 3 (L-points at the corners), bands 1 and 4 (Γ -points at the corners). The bottom panel shows the Fermi surface 100 ($k_x = 0$) cross-section. The widths of the lines correspond to actual exchange splitting for magnetization $M = 0.2 \mu_B$.

The coupling constant, defined as $\lambda_{ep} = 2 \sum_{\mathbf{k}\alpha} \delta(\varepsilon_{\mathbf{k}\alpha} - E_F) (d\varepsilon_{\mathbf{k}\alpha}/du)^2 / 2M\omega^2$, where $\sum_{\mathbf{k}\alpha} \delta(\varepsilon_{\mathbf{k}\alpha} - E_F)$ is the density of states at the Fermi level per spin, M is the ionic mass, ω is the phonon frequency, and $(d\varepsilon_{\mathbf{k}\alpha}/du)^2$, is $\lambda_{ep} = 0.115$. Note that this mode is triple degenerate at Γ , so the total contribution to λ_{ep} from this mode is ≈ 0.35 . However, since we expect that all rattling modes of Zr would couple at a general point in the Brillouin zone with a similar strength, we estimate the total contribution from the six rattling modes to be ≈ 0.7 . Finally, the remaining 12 modes (especially the two rather soft E_u modes, which we expect to couple less with electrons, should bring a smaller, but finite contribution to the total λ_{ep} , so we take as a rough estimate $\lambda_{ep} \approx 1$. With a Coulomb pseudopotential $\mu^* = 0.1$, the McMillan formula yields $T_c \approx 10$ K. This is a reasonable number since spin fluctuations should reduce T_c (and eventually eliminate superconductivity) in this scenario. This is also consistent with the transport coupling constant extracted from the linear part of the resistivity vs. temperature dependence [19] of ZrZn_2 single crystals [20], $\lambda_{tr} = 1.4$. Assuming that $\lambda_{tr} \approx \lambda_{ep} + \lambda_{es}$, where λ_{es} characterizes coupling with spin fluctuations, we get $\lambda_{es} \approx 0.4$, and the modified McMillan formula then gives $T_c = (\omega_{ph}/1.2) \exp[-1.02(1 + \lambda_{ep} + \lambda_{es}) / (\lambda_{ep} - \lambda_{es} - \tilde{\mu}^*)] \approx$

0.3 K. Here $\tilde{\mu}^* = \mu^*(1 + 0.62\lambda_{ep} + 0.62\lambda_{es})$. On the other hand, the specific heat coefficient of $47 \text{ mJ mol}^{-1}\text{K}^{-2}$, reported in Ref. [1], corresponds to mass renormalization 4.1, considerably larger than $(1 + \lambda_{ep} + \lambda_{es}) = 2.4$. [21]

Another interesting observation is that the topology of the Fermi surface changes so sharply with the chemical potential, that the calculated coupling constant λ_{ep} is very sensitive to the exact position of the Fermi level in the band structure. In Fig.4 we show its dependence on the Fermi level position. We observe that if the Fermi level were 20 meV, λ_{ep} would be 50% larger. This unusual sensitivity is only partially accounted for by the structure of the density of states (Fig.4). Of course, the tendency to magnetism also strongly depends on the position of the Fermi level.

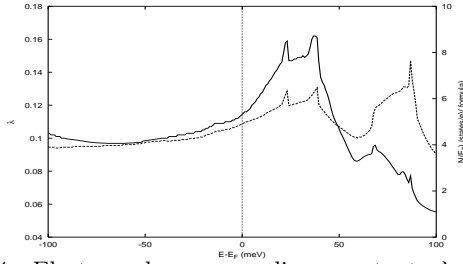


FIG. 4. Electron-phonon coupling constant, λ_{ep} , for one T_{2g} mode as a function of the Fermi level position. Solid line is λ_{ep} , dashed line is density of states.

In conclusion, we report accurate calculations of the electronic structure and the zone-center phonons in ZrZn_2 both in para- and ferromagnetic state. The recently observed superconductivity is compatible with any of the three scenarios: (1) sample inhomogeneity leading to separation of superconductivity and magnetism in real space, (2) coexistence of ferromagnetism and inhomogeneous s-wave superconducting state (Fulde-Ferrell-Larkin-Ovchinnikov state), and (3) triplet spin-fluctuation induced superconductivity. Further experiments should be able distinguish between these three scenarios, since they predict rather different thermodynamic behavior: an exponential BCS-like temperature dependencies vs. a finite residual density of states vs. a power law due to the gap nodes.

This work was supported by ONR and the ASC super-computer center.

-
- [1] C. Peiderer, M. Uhlarz, S.M. Hayden, R. Vollmer, H.v.Lohnneysen, N.R. Bernhoeft and C.G. Lonzarich, Nature **412**, 58 (2001).
[2] B. T. Matthias and R.M. Bozorth, Phys. Rev. **109**, 604 (1958).
[3] V. L. Ginzburg, Sov. Phys. JETP **4**, 153 (1957).

- [4] D. Fay and J. Appel, Phys. Rev. **B 22**, 3173 (1980).
[5] H.G. Cordes, K. Fischer, and F. Pobell, Physica B & C **107**, 531 (1981).
[6] T.F. Smith, J.A. Mydosh, and E.P. Wohlfarth, Phys. Rev. Lett **27**, 1732 (1971).
[7] P. Fulde and R. A. Ferrell, Phys. Rev. **135**, A550 (1964). A. I. Larkin and Yu. N. Ovchinnikov, Zh. Eksp. Teor. Fiz. **47**, 1136 (1964) [Sov. Phys. JETP **20**, 762 (1965)].
[8] S. Ogawa, Physica B & C **119B**, 68 (1983).
[9] L. Hedin, and B. I. Lundqvist, J. Phys. C **4**, 2064 (1971).
[10] D.J. Singh, *Planewaves, Pseudopotentials and the LAPW Method* (Kluwer Academic, Boston, 1994).
[11] D. Singh, Phys. Rev. B **43**, 6388 (1991).
[12] M. Huang, H.J.F. Jansen, and A.J. Freeman, Phys. Rev. B **37**, 3489 (1988).
[13] G. Santi, S.B. Dugdale, and T. Jarlborg, cond-mat/0107304 (2001).
[14] Note, however, that the Fermi surface topology is quite sensitive to the position of the Fermi level; shifting the Fermi level by 40 meV in *either* direction makes the Hall coefficient change sign from electron-like to hole-like. This suggests nontrivial temperature dependence of the Hall coefficient.
[15] Note that the hopping in the fcc lattice is $dd\sigma$, while in the diamond structure it is an average of $dd\sigma$ and $dd\pi$ hoppings, which gives an additional increase in the bandwidth, and that the diamond structure possess a pseudo-gap due to the bonding-antibonding splitting of the two Zr, thus increasing the density of states at the Fermi level.
[16] This also can be seen in the shape of this band along the Γ -X line: in the nearest-neighbor Zr-Zr model, this band should be cosinusoidal, but a noticeable second harmonic component is clearly seen in Fig.2. This is due to the Zn-assisted effective second neighbor hopping.
[17] T.R. Kirkpatrick, D. Belitz, T. Vojta, and R. Narayanan, cond-mat/0105627 (2001).
[18] Standard frozen-phonon technique was employed for the lattice dynamics calculations; both total energies and forces were used for constructing the dynamical matrix.
[19] L.W.M. Scheurs, H.M. Weijers, A.P.J. van Deursen, and A.R. de Vroomen, Mat. Res. Bull., **24**, 1141 (1989).
[20] Note that the resistivity reported in Ref. [19] starts to deviate from the linear behavior already at $T \gtrsim 150 \text{ K}$. This can be attributed to the “resistivity saturation” due to the proximity to the Ioffe-Regel localization. Indeed, the mean free path at $T = 150 \text{ K}$, computed using the LSDA Fermi velocity, is only twice longer than the lattice parameter.
[21] This analysis is based on the assumption that λ_{es} is the same above and below the Curie temperature. This is partially justified by the fact that $\rho(T)$ does not show any anomaly at T_C . [19]

TABLE I. Zone center phonon modes in ZrZn_2

mode	T_{2g}^a	T_{1u}^b	E_u^c	T_{1u}^d	A_{1u}^e	T_{2u}^c
character	Zr	mostly Zr	Zn	mostly Zn	Zn	Zn
$\omega \text{ (cm}^{-1}\text{)}$	120	133	142	182	250	277

^a Out-of-phase Zr rattling; ^b In-phase Zr rattling; ^c Zn breathing (the tetrahedra breathe out of phase with each

other); ^dMixed mode; ^eZn breathing (all three tetrahedra breathe in phase).